# PLOS ONE

# Temperature-dependent responses of the hard corals *Acropora* sp. and *Pocillopora verrucosa* to molecular hydrogen

**Malte Ostendarp**[1]*, **Mareike de Breuyn**[1], **Yusuf C. El-Khaled**[2], **Neus Garcias-Bonet**[2], **Susana Carvalho**[2], **Raquel S. Peixoto**[2], **Christian Wild**[1]

**1** Marine Ecology Department, Faculty of Biology and Chemistry, University of Bremen, Bremen, Germany, **2** Division of Biological and Environmental Science and Engineering, King Abdullah University of Science and Technology, Thuwal, Saudi Arabia

* maos@uni-bremen.de
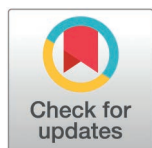
## Abstract

Coral reefs are increasingly threatened by mass bleaching events due to global ocean warming. Novel management strategies are urgently needed to support coral survival until global efforts can mitigate ocean warming. Given the strong antioxidant, anti-inflammatory and anti-apoptotic properties of molecular hydrogen, our study explores its potential to alleviate the negative effects of heat stress on corals. We investigated the ecophysiological responses of two common hard corals (*Acropora* sp. and *Pocillopora verruco*sa) from the Central Red Sea under ambient (26 °C) and elevated seawater temperatures (32 °C), with and without hydrogen addition (~ 150 µM H$_2$) over 48 h. Our results showed that at 32 °C without hydrogen addition, *P. verrucosa* exhibited high temperature tolerance, whereas *Acropora* sp. showed significant reductions in photosynthetic efficiency and maximum electron transport rate compared to the ambient condition (26 °C). The addition of hydrogen at 32 °C increased the maximum electron transport rate of *Acropora* sp. by 28%, maintaining it at levels compared to those at 26 °C. In contrast, the addition of hydrogen at 26 °C caused a significant decrease in the photophysiology of both *Acropora* sp. and *P. verrucosa*. This suggests that the short-term response of the coral holobiont to molecular hydrogen is temperature-dependent, potentially benefiting the coral holobiont under heat stress, while impairing the photophysiology under ambient temperatures. Our findings therefore provide the foundation for future long-term studies uncovering the mechanisms behind molecular hydrogen, potentially informing the development of new management strategies to enhance coral resilience to ocean warming.

## Introduction

Coral reefs are among the most biodiverse and productive ecosystems worldwide [1]. They provide humankind with a diverse range of essential ecosystem services [1], on which millions of livelihoods depend [2]. However, coral reefs are currently in serious decline [3,4], as a result of many different local and global anthropogenic and natural threats, including local pollution, overfishing, and global warming [5–9].

Although many of these threats are currently identified and partially addressed, climate change continues at a rapid pace with minimal progress made towards mitigation [10,11]. In association with the onset of El Niño in 2023 [12], new ocean temperature records are emerging [13,14], greatly increasing the probability and frequency of mass coral bleaching and mortality events worldwide [10,15–17]. Direct actions and strategies are urgently needed to further prevent the rapid degradation of these highly valuable ecosystems and buy time for coral reefs until climate change becomes manageable by global efforts [18].

Climate change-associated shifts in physical and biogeochemical conditions are widely recognized to induce coral bleaching, which is the loss of the coral's endosymbiotic algae (Symbiodiniaceae) that often represent the main energy source of the coral host [19,20]. Novel intervention approaches could therefore aim to target physiological cascades associated with coral bleaching, particularly those initiated by heat stress, offering a promising approach for improving coral resilience. Several prominent cascades have been proposed, highlighting the roles of both nitrogen availability and oxidative stress [20]. One cascade involves the disruption of a nitrogen-limited state, essential for maintaining a stable symbiosis between the coral host and its algae, by an increased nitrogen availability [19,21,22]. Another cascade involves the increased generation of reactive oxygen species (ROS) and reactive nitrogen species (RNS), primarily triggered by temperature and light stress, that overwhelms the coral's antioxidative capacity and potentially induces a stress response ultimately resulting in coral bleaching as proposed by the "Oxidative Theory" [23,24].

In this context, molecular hydrogen might offer an effective treatment to mitigate coral bleaching. Due to hydrogen's strong antioxidant, anti-inflammatory and anti-apoptotic characteristics, it has been used as a preventive and therapeutic agent in human medicine [25–30]. As a strong antioxidant, molecular hydrogen selectively reduces hydroxyl radicals and peroxynitrite, which are among the most harmful ROS/RNS [25]. In contrast, other ROS/RNS with a potentially beneficial physiological role are not affected by molecular hydrogen [25,29,30]. Since molecular hydrogen is also able to rapidly diffuse across membranes, it can successfully penetrate cell organelles [25] and scavenge ROS/RNS inside the cytoplasm and mitochondria. In addition, molecular hydrogen is proposed to inhibit the generation of ROS/RNS by preventing leakage of electrons from the electron transport chain [30], regulate gene expression [29], increase overall antioxidant capacity [31,32] and upregulate the heat shock response [33].

Based on these previously observed effects of molecular hydrogen in mammals including humans and rats [25–30], here we provide first insights into the potential effects of molecular hydrogen on the coral holobiont. Our objective was to assess if molecular hydrogen affects the ecophysiology of corals under heat stress. Considering its antioxidant, anti-inflammatory and anti-apoptotic properties [25–30], we hypothesize that molecular hydrogen minimizes negative effects of heat stress.

To address the research question and associated hypothesis, we experimentally examined the short-term effect (48 h) of hydrogen-enriched seawater under ambient temperature and heat stress on the two common and widely distributed hard corals *Acropora* sp. and *P. verrucosa* from the Central Red Sea. For this purpose, we analyzed several physiological parameters related to bleaching phenotype, photosynthetic capacity and holobiont phenotype. For the bleaching phenotype, Symbiodiniaceae cell density, chlorophyll a and c2 concentrations and primary production ($P_{net}$ and $P_{gross}$) were analyzed. These parameters can directly indicate a loss of endosymbionts and pigmentation, which are associated with reduced primary production and serve as key indicators of coral bleaching [34].

Building on the assessment of the bleaching phenotype, we further evaluated the photosynthetic capacity by measuring the photosynthetic efficiency, maximum electron transport

rate (ETR$_{max}$), and minimum saturating irradiance (E$_k$) with ETR$_{max}$ indicating the maximum capacity of the electron transport chain and E$_k$ reflecting the light intensity at which photosynthesis becomes saturated [35]. These parameters therefore provide insight into the functional state of the photosynthetic apparatus [35], with temperature-induced shifts indicating the loss of healthy endosymbionts or revealing disruptions within the photosynthetic machinery, even before the loss of endosymbionts occurs [36,37].

At the holobiont phenotype, we assessed respiration rates (R), which serve as a proxy for the metabolic demand typically increasing under stress [34]. By connecting these parameters, we generated a comprehensive overview of coral holobiont health, identifying the physiological responses of *Acropora* sp. and *P. verrucosa* to short-term heat stress and evaluating the potential role of hydrogen in minimizing temperature-induced negative effects.

## Materials and methods

### Coral collection and experimental preparation

To assess the short-term effect of hydrogen addition on the coral holobiont, two common Red Sea coral species, *Acropora* sp. and *P. verrucosa*, were selected. *Acropora* fragments were collected based on morphological characteristics (*Acropora* cf. *hemprichii*). However, due to the complex taxonomy within the genus *Acropora*, we decided to conservatively refer to *Acropora* sp. Coral fragments were sampled by SCUBA diving near the "Coral Probiotics Village" at Al Fahal Reef (22°18'19.1''N, 38°57'55.0''E), located about 20 km off the King Abdullah University of Science and Technology, Thuwal, in the Saudi Arabian coast of the Red Sea. Permits were obtained from the Institutional Biosafety and Bioethics Committee of the King Abdullah University of Science and Technology (IBEC protocol number 22IBEC003_v4).

A total of six colonies per species were tagged at a depth of approximately 10 m to allow the identification and resampling of the same colonies during the experiment duration. On each sampling day, two coral fragments per colony measuring about 3 - 5 cm in length were collected using pliers along with 90 L of seawater in water containers. Due to laboratory space limitations, it was not possible to run all incubations simultaneously. Therefore, short-term incubations (48 h) were carried out on four different days, with each day randomly assigned to a specific temperature and treatment group (CT26, CT32, H$_2$26, H$_2$32). These incubations were conducted within the shortest possible timeframe lasting from 07$^{th}$ to 23$^{rd}$ of March 2023 to minimize the impact of potential seasonal changes. For each incubation, the respective coral fragments were collected on the same day. Our decision for this approach was driven by the need for controlled environmental conditions, the feasibility of treatment application, and the aim to capture a large biological variability of corals. Consequently, our setup was restricted to one tank per treatment and species, as it was intended to apply heat stress and treatments over a 48-h period rather than for extended coral maintenance. Reef environmental parameters, including seawater temperature and salinity, were recorded during this period (S1 File) using a multiparameter conductivity, temperature and depth (CTD) sensor (Ocean Seven 310, Idronaut, Italy).

### Experimental design

After collection, the coral fragments were transported to the laboratory in transparent sampling bags within a plastic box containing ambient seawater and a portable aquarium pump to ensure aeration. Immediately after arrival, all 24 fragments were attached to custom-made stands marked with colored stripes for the respective colony and placed inside two plastic aquaria, one for each species, filled with 30 L of seawater collected from the reef. The aquaria were equipped with an aquarium pump and a heater connected to a thermostat while natural

lighting was simulated with a LED lamp replicating a 12 h light/dark-cycle (PAR ~ 200 µmol m$^{-2}$ s$^{-1}$, salinity 39.0 ± 1.0 ‰, temperature ambient 26.0 ± 0.5 °C/ increased 32 ± 0.5 °C). On each sampling day, all fragments were incubated for 48 h in one treatment (CT = control, H$_2$ = hydrogen-enriched) and under one temperature condition (ambient = 26 °C, heat stress = 32 °C) resulting in four different groups: CT26, CT32, H$_2$26, H$_2$32.

To increase the hydrogen concentration, a hydrogen water generator was used (Hydrogen-rich Water Cup, ABS-FQ-02, Aukewel) that produced 240 mL of hydrogen-enriched distilled water with a concentration of ~ 3 ppm each cycle according to test reports provided by the manufacturer. In all groups, 10% of the total seawater was exchanged at the start and after 24 h with artificial seawater created with MilliQ-water and marine sea salt (Red Sea salt, Red Sea) at the respective temperature. In the hydrogen treatments, the artificial seawater was previously hydrogen enriched resulting in a theoretical hydrogen concentration of ~ 0.3 ppm (~ 150 µM). However, as molecular hydrogen is barely soluble [29] and is constantly released, we can only assume a hydrogen spike at the start and after 24 h of the experiment. After the first water exchange, the temperature was ramped in the heat stress groups from 26 °C to 32 °C within 2 h. Temperature and salinity were checked consistently throughout the experiment using a handheld sensor (YSI professional plus handheld multiparameter meter) to potentially adjust temperature and salinity. Due to a malfunctioning heater in the *P. verrucosa* aquarium during the CT32 group, the water temperature decreased in the first 12 h after the ramping to 28 °C and was then ramped up back to 32 °C within 2 h.

Following the 48 h incubation period, several response parameters related to coral physiology and the overall coral holobiont health were assessed as proxies of the stress state. Survival and bleaching of every fragment were visually analyzed. Then, six fragments per species were used to measure photosynthesis and respiration rates, photosynthetic efficiency (*Fv/Fm*) and rapid light curves (RLC). The remaining six fragments per species were frozen for further analyses of Symbiodiniaceae cell density and chlorophyll a and c2 content. To normalize response parameters to the size of the coral fragments, the surface area was measured using 3D models in Autodesk ReCap Photo (version 23.1.0) according to Lavy et al. [38] and Tilstra et al. [39]. For this purpose, at least 20 photographs were taken from all sides of the fragment. Photographs were taken after the incubation to avoid stressing the corals beforehand. From these photographs 3D models were created and sliced to only include the fragment surface. The surface area in cm$^2$ was then calculated by the program using a reference scale placed on each picture.

### Data collection

**Survival and bleaching.** Survival and bleaching of all fragments were visually assessed directly after the 48 h incubations. Fragments were classified as dead if 100% tissue loss was visible.

**Photosynthesis and respiration.** Six fragments per species were placed on custom-made stands into 1 L jars filled with the respective treatment water and sealed airtight without any air bubbles inside to measure oxygen fluxes according to Tilstra et al. [39] and Mezger et al. [40]. In addition, three 1 L jars per aquaria were filled with treatment water excluding any coral fragments to account for background photosynthesis and respiration rates. Briefly, all jars were placed into a water bath equipped with a heater connected to a thermostat to maintain the temperature at the respective temperature condition. Magnetic stirrers (~ 200 rpm) placed onto stirring plates (magnetic stirrer HI 200M, Hanna instruments) ensured a constant water flow and homogenous conditions inside the jars. Initially, all fragments and seawater blanks were light-incubated for 90 min (PAR ~ 200 µmol m$^{-2}$ s$^{-1}$) and afterwards

dark-incubated for 60 min. The variation in light and dark incubation period ensured that the oxygen concentration remained within a reliable range. Oxygen concentrations were measured at the start and end of the light and dark incubation using an oxygen probe (Multi 3500i handheld multimeter, WTW and YSI professional plus handheld multiparameter meter). Two calibrated oxygen probes were used in between treatments due to technical difficulties (Multi 3500i handheld multimeter, WTW was used for the $H_2 26$ group and YSI professional plus handheld multiparameter meter for the CT26, CT32 and $H_2 32$ groups).

To calculate net photosynthesis ($P_{net}$) and respiration (R) rates, start and end oxygen concentrations of the light and dark incubations were subtracted, respectively. $P_{net}$ and R were then normalized by the surface area of each fragment, total volume of the incubation jar, total incubation time and the background photosynthesis and respiration rates.

Using $P_{net}$ and R, the gross photosynthesis ($P_{gross}$) was then calculated according to following formula:

$$P_{gross} = P_{net} + |R|$$

**Photosynthetic efficiency and rapid light curves.** Photosynthetic efficiency was measured directly after the dark incubation using an Imaging-PAM (model IMAG-K7, Walz GmbH) according to Ralph and Gademann [35] and Ralph et al. [41], as the corals were already dark-adapted for > 30 min. For each fragment, the dark level fluorescence yield (*F0*) and the maximum fluorescence yield (*Fm*) were measured using the following PAM settings: gain = 2, damp = 2, saturation intensity = 7, saturation width = 4 and measuring light intensity = 7. The optimal PSII quantum yield (*Fv/Fm*) was calculated for five points randomly placed on the coral fragment. In addition, a rapid light curve (RLC) was generated afterwards for the same five points through an exposure of twelve light-series with increasing irradiance from 0 to 702 µmol photons $m^{-2}$ $s^{-1}$. Between the twelve light-series, the fragments were illuminated with the respective actinic light for 20 s, each ended by a saturation pulse. Through all of the five RLCs per fragment one model was fitted according to Platt et al. [42] using the following equation:

$$y = ps \times \left(1 - e^{\frac{-x \times \alpha}{ps}}\right) \times e^{\frac{-x \times \beta}{ps}}$$

For the model, values of 0 µmol electrons $m^{-2}$ $s^{-1}$ which were recorded at higher irradiances than 0 µmol photons $m^{-2}$ $s^{-1}$ were excluded in advance. This exclusion was made due to the model's sensitivity as the variables of interest were chosen prior to this range. To determine the variables ps, $\alpha$ and $\beta$, a pseudo-random search algorithm was run within the package *phytotools v.1.0* [43] in the program R *v.4.3.0* [44]. The maximum electron transport rate ($ETR_{max}$) and minimum saturating irradiance ($E_k$) were calculated using the determined variables as follows:

$$ETR_{max} = ps \times \frac{\alpha}{\alpha + \beta} \times \left(\frac{\beta}{\alpha + \beta}\right)^{\frac{\beta}{\alpha}}$$

$$E_k = \frac{ETR_{max}}{\alpha}$$

**Symbiodiniaceae cell densities and chlorophyll concentrations.** Coral tissue was removed using an airbrush filled with 10 mL distilled water. The tissue slurry was collected in a 15 mL falcon tube to measure the total volume. In between fragments, the airbrush was

cleaned with 70% ethanol. After airbrushing, the slurries were frozen at -20 °C until further analysis.

To assess the Symbiodiniaceae cell density, a total of 100 μL tissue slurry was thawed and vortexed (analog vortex mixer, VWR). Each sample was then centrifuged for 5 min at 8000 rpm (centrifuge 5424R, Eppendorf). Subsequently, the supernatant was discarded and 1 mL of MilliQ-water was added to the pellet. After dissolving the pellet and homogenizing the mixture using a vortex (analog vortex mixer, VWR), the sample was pipetted on a cell strainer with a 30 μm mesh size to remove larger cells. Following filtration, 200 μL per sample were placed in duplicates in a microplate well. Symbiodiniaceae cell density was then measured using a flow cytometer (Accuri C6 Flow Cytometer, BD). Between samples, a washing and agitating cycle was run and in between three samples, the plate was vortexed to ensure a homogenous mixture. Each sample was run for 2 min and if the events/s recorded by the flow cytometer exceeded 1000, the sample was diluted with MilliQ-water and rerun. The initial count was normalized to the volume sampled by the flow cytometer, surface area, dilution and slurry volume.

A total of 1 mL tissue slurry was thawed and used to measure chlorophyll a and c2 in duplicates. Each sample was centrifuged (centrifuge 5424R, Eppendorf) for 5 min with 5000 rpm at 4 °C and afterwards the supernatant was discarded. To extract chlorophyll a and c2, 2 mL of 90% acetone was added to each sample. The samples were then sonicated for 10 min and dark-incubated for 24 h at 4 °C. Following 24 h, 200 μL of each sample were transferred in duplicates in a micro-plate well. Additionally, three 200 μL 90% acetone blanks were placed on each microplate well to normalize values afterwards. The chlorophyll a and c2 concentrations were assessed by measuring the absorbance at 630 nm ($E_{630}$) and 663 nm ($E_{663}$) using a spectrophotometer (Multiskan SkyHigh microplate spectrophotometer v.1.0.70.0, Thermo Fisher Scientific). Final values were calculated according to Jeffrey and Humphrey [45] and normalized to the surface area, the slurry volume and the averaged absorbance of the blanks. As Jeffrey and Humphrey [45] assumed a path length of 1 cm path which is inaccurate for a microplate well, all values were additionally divided by 0.555. Final chlorophyll a and c2 concentrations were also normalized by Symbiodiniaceae cell density.

**Statistical analyses.** The statistical analyses were conducted in the PRIMER-E software *v.6.1.18* [46] with the PERMANOVA + add on *v.1.0.8* [47] using a permutational multivariate analysis of variance (PERMANOVA). The type III (partial) PERMANOVAs with unrestricted permutations of raw data (999 permutations) including a Monte Carlo test were performed on a resemblance matrix created with the Euclidean distance of the previously normalized data. Two-factorial (factors: temperature [T; two levels: 26 °C, 32 °C], treatment [Tr; two levels: Control, Hydrogen]) PERMANOVAs were carried out for each species on the variables within the oxygen fluxes ($P_{net}$, R, $P_{gross}$), photosynthetic efficiency (*Fv/Fm*), rapid light curves (α, ps/$ETR_{max}$, $E_k$), chlorophyll ($Chl_a$, $Chl_{c2}$) and Symbiodiniaceae cell density (S1 File). The results were considered significant below a p-value of 0.05. If the interaction effect (T x Tr) was significant, PERMANOVA pairwise tests including a Monte Carlo test were conducted within the temperature and treatment level.

The RLC models and all graphs were created in R *v.4.3.0* [44] using the packages *phytotools v.1.0* [43], *tidyverse v.2.0.0* [48], *ggpubr v.0.6.0* [49] and *rstatix v.0.7.2* [50]. All plots and values represent the mean value and the respective standard error (MEAN ± SE). The raw data is provided in the supporting information (S1 Data).

## Results

### Survival and bleaching

Neither *Acropora* sp. nor *P. verrucosa* exhibited visual signs of mortality or bleaching across all treatments (CT26, CT32, H₂26, H₂32).

## Photosynthesis and respiration

Gross photosynthesis and respiration rates of *Acropora* sp. were significantly affected by temperature (Fig 1A, PERMANOVA, p (respiration) = 0.004, p (gross photosynthesis) = 0.049). Under heat stress (CT32 and $H_2$32), gross photosynthesis and respiration rates were significantly increased compared to ambient seawater temperatures (CT26 and $H_2$26).

In contrast, net and gross photosynthesis as well as respiration rates of *P. verrucosa* were significantly affected by an interaction between treatment and temperature (Fig 1B, PERMANOVA, p (respiration) = 0.001, p (net photosynthesis) = 0.019, p (gross photosynthesis) = 0.003). The addition of hydrogen at ambient seawater temperatures ($H_2$26) caused a significant decline in net photosynthesis, gross photosynthesis, and respiration rates of *P. verrucosa* compared to CT26 (Fig 1B, pairwise PERMANOVA, p (respiration) = 0.013, p (net photosynthesis) = 0.001, p (gross photosynthesis) = 0.003). However, the addition of hydrogen under heat stress ($H_2$32) resulted in significantly higher respiration, net photosynthesis, and gross photosynthesis rates of *P. verrucosa* compared to $H_2$26 (Fig 1B, pairwise PERMANOVA, p (respiration) = 0.001, p (net photosynthesis) = 0.011, p (gross photosynthesis) = 0.001).
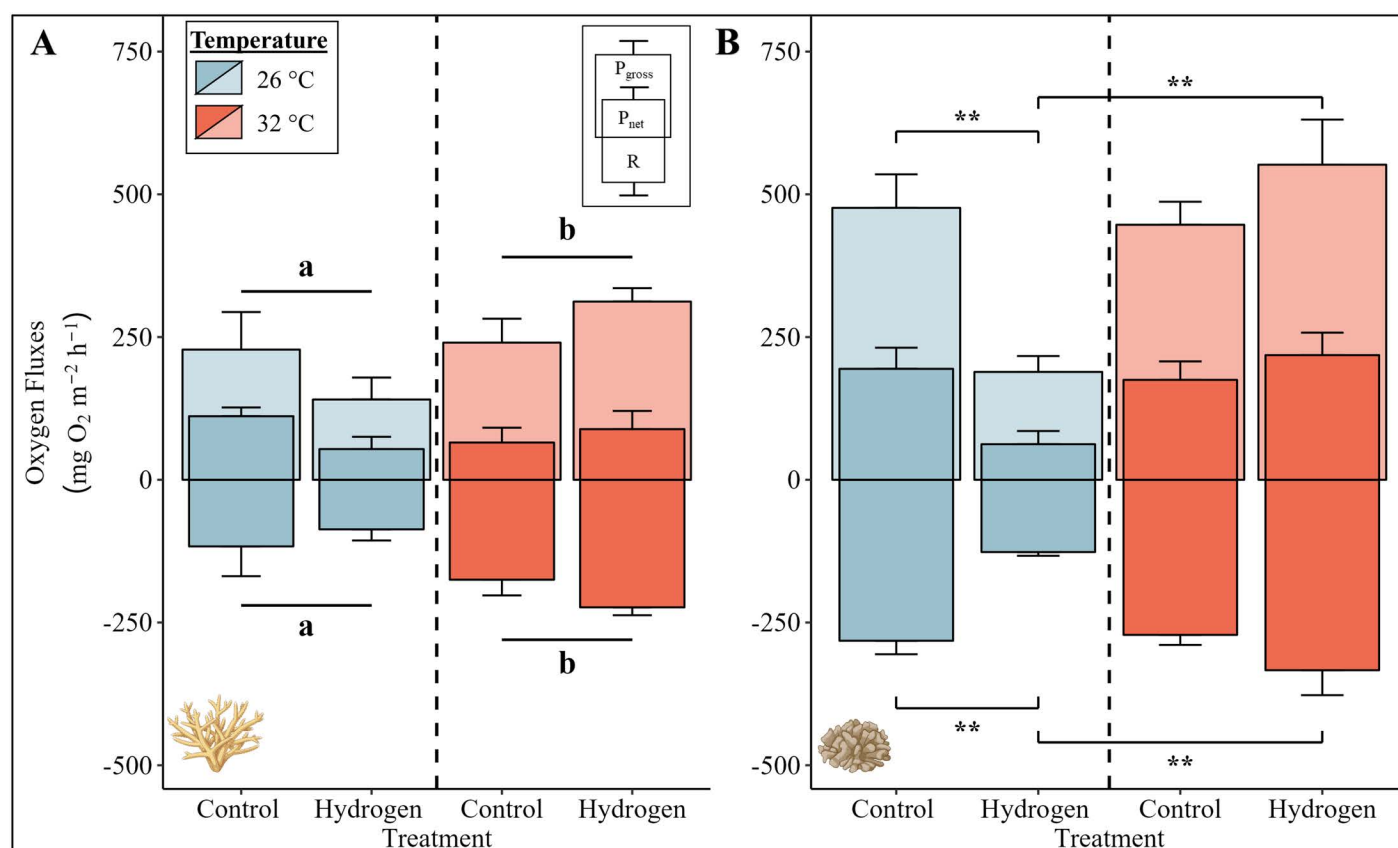


**Fig 1. Photosynthesis and respiration rates of (A) *Acropora* sp. and (B) *P. verrucosa* for the four groups.** Mean net and gross photosynthesis ($P_{net}$ and $P_{gross}$) and respiration (R) rates are visualized by bars with error bars indicating the respective standard error (SE) of six replicates per group (except for four in the CT26 group *Acropora* sp. and five in the CT32 group *P. verrucosa* due to a measurement error). The color of the bars indicates the temperature condition (blue = 26 °C, red = 32 °C). For *Acropora* sp. (A), a significant temperature main effect according to the PERMANOVA with Monte-Carlo test is presented with letters ([a/b] p < 0.05; above bar: $P_{gross}$, below bar: R) and black lines grouping the temperature conditions. For *P. verrucosa* (B), pairwise PERMANOVAs with Monte-Carlo tests were conducted as the interaction effect between temperature and treatment was significant. Significant differences in between treatments are illustrated with asterisks (* p < 0.05, ** p < 0.01; above bar: $P_{gross}$, below bar: R). Exact p-values are presented in supplementary material (S1 File). Coral illustrations were created with BioRender.com.

https://doi.org/10.1371/journal.pone.0308894.g001

These photosynthesis and respiration rates at $H_2$32 were resembling those observed in both control groups at ambient (CT26) and heat stress (CT32) conditions.

## Photosynthetic efficiency and rapid light curves

Similar to the photosynthesis and respiration rates, the photosynthetic efficiency of *Acropora* sp. was significantly affected by temperature ([Fig 2A](#), PERMANOVA, p = 0.003). Heat stress (CT32 and $H_2$32), however, caused a significant reduction in the photosynthetic efficiency in comparison to the treatments without heat stress (CT26 and $H_2$26).

In comparison, the photosynthetic efficiency of *P. verrucosa* was not affected by temperature or treatment.

The $ETR_{max}$ and $E_k$ of *Acropora* sp., derived from the RLCs ([Fig 3A](#)), were both significantly affected by an interaction between temperature and treatment ([Fig 3B](#) and [3C](#), PERMANOVA, p ($ETR_{max}$) = 0.002, p ($E_k$) = 0.019). $ETR_{max}$ of *Acropora* sp. significantly decreased in the heat stress treatment CT32 ([Fig 3B](#), pairwise PERMANOVA, p = 0.003) and in the hydrogen treatment $H_2$26 ([Fig 3B](#), pairwise PERMANOVA, p = 0.001) compared to the control treatment CT26. However, $ETR_{max}$ remained significantly higher for *Acropora* sp. in the combined treatment of heat stress and hydrogen addition ($H_2$32) than in the CT32 ([Fig 3B](#), pairwise PERMANOVA, p = 0.044) and $H_2$26 treatments ([Fig 3B](#), pairwise PERMANOVA, p = 0.036) and comparable to the $ETR_{max}$ observed in the CT26 treatment. Similar to the decrease in the $ETR_{max}$, $E_k$ values of *Acropora* sp. also declined significantly in the presence of hydrogen-enriched seawater ($H_2$26) compared to the control group CT26 ([Fig 3C](#), pairwise PERMANOVA, p = 0.008).

While the $ETR_{max}$ of *P. verrucosa*, derived from the RLCs ([Fig 4A](#)), remained unaffected by heat stress or hydrogen addition ([Fig 4B](#)), $E_k$ was significantly affected by temperature ([Fig 4C](#), PERMANOVA, p = 0.018) causing a significant decrease in both heat stress treatments (CT32 and $H_2$32) compared to the treatments without heat stress (CT26 and $H_2$26).
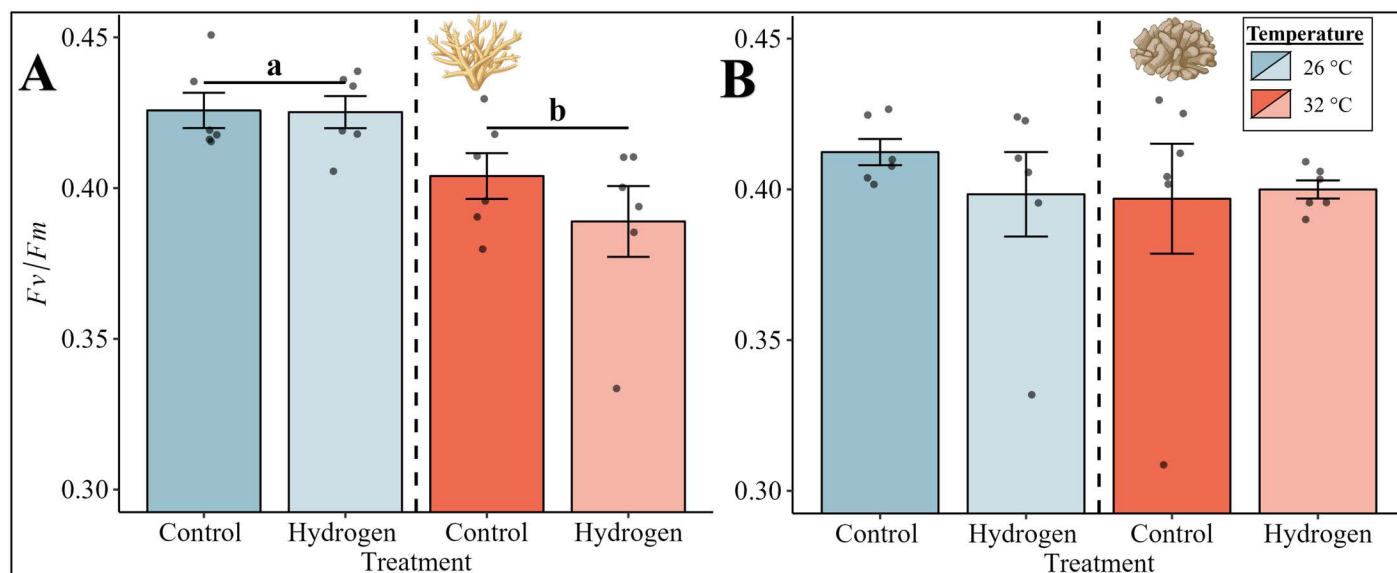


**Fig 2. Photosynthetic efficiency (*Fv/Fm*) of (A) *Acropora* sp. and (B) *P. verrucosa* for the four groups.** Mean photosynthetic efficiency is visualized by bars with error bars indicating the respective standard error (SE) of six replicates per group. The color of the bars indicates the temperature condition (blue = 26 °C, red = 32 °C). A significant temperature main effect according to the PERMANOVA with Monte-Carlo test (p < 0.05) is presented with letters and black lines grouping the temperature conditions. Exact p-values are presented in supplementary material ([S1 File](#)). Coral illustrations were created with BioRender.com.

https://doi.org/10.1371/journal.pone.0308894.g002
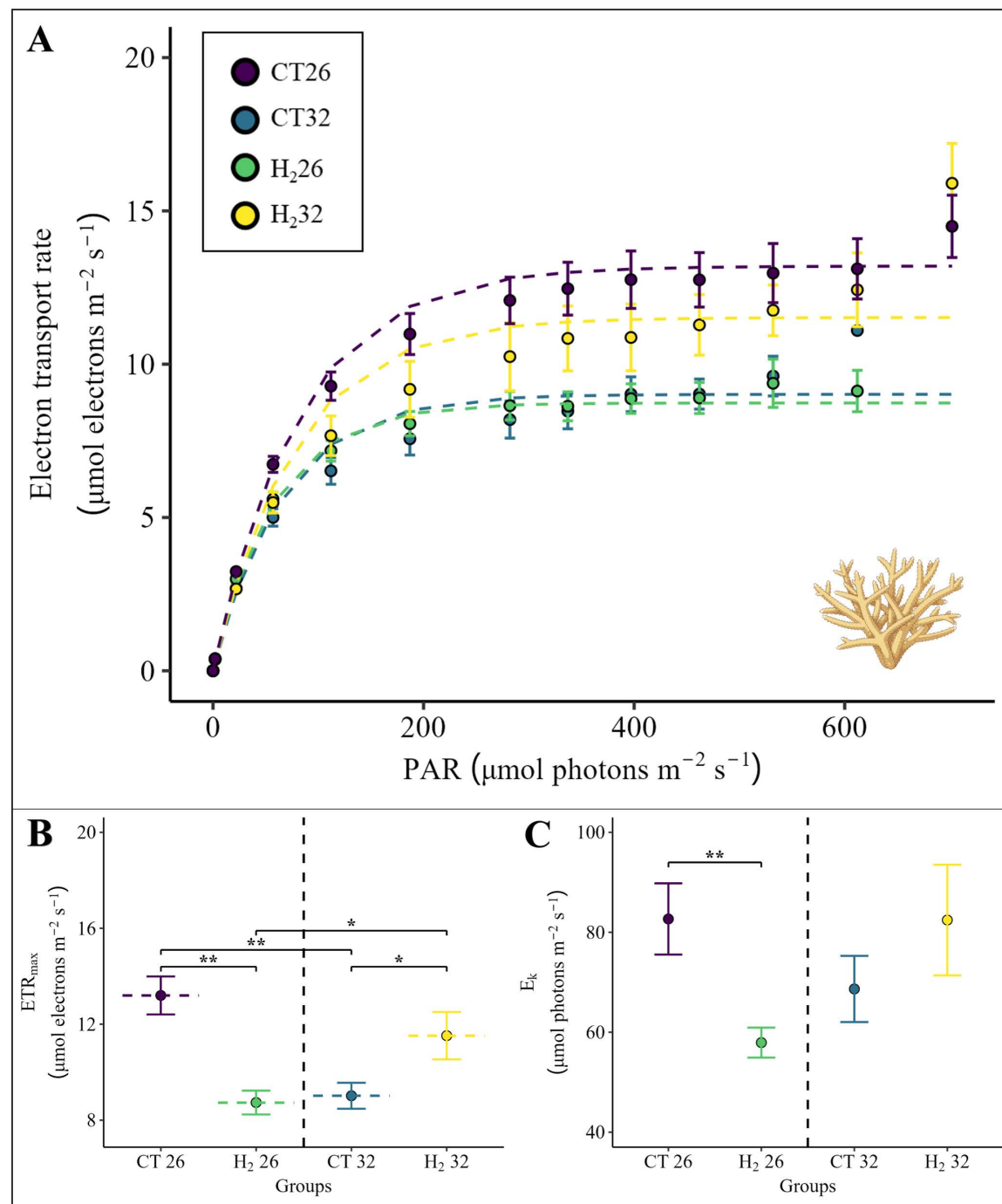
**Fig 3. (A) Rapid light curves, (B) maximum electron transport rates (ETR$_{max}$) and (C) minimum saturating irradiances (E$_k$) derived from the model fitted according to Platt et al. [42] for all four groups belonging to** *Acropora* **sp.** The rapid light curves and the respective ETR$_{max}$ and E$_k$ values are calculated as the mean of six replicates per group (S1 File). The four groups are illustrated with different colors. Points indicate the mean value and error bars the respective standard error (SE). Pairwise PERMANOVAs with Monte-Carlo tests were conducted if the interaction effect between temperature and treatment was significant and are illustrated with asterisks indicating a significant difference ( * p < 0.05, ** p < 0.01). Exact p-values are presented in supplementary material (S1 File). Coral illustration was created with BioRender.com.

https://doi.org/10.1371/journal.pone.0308894.g003
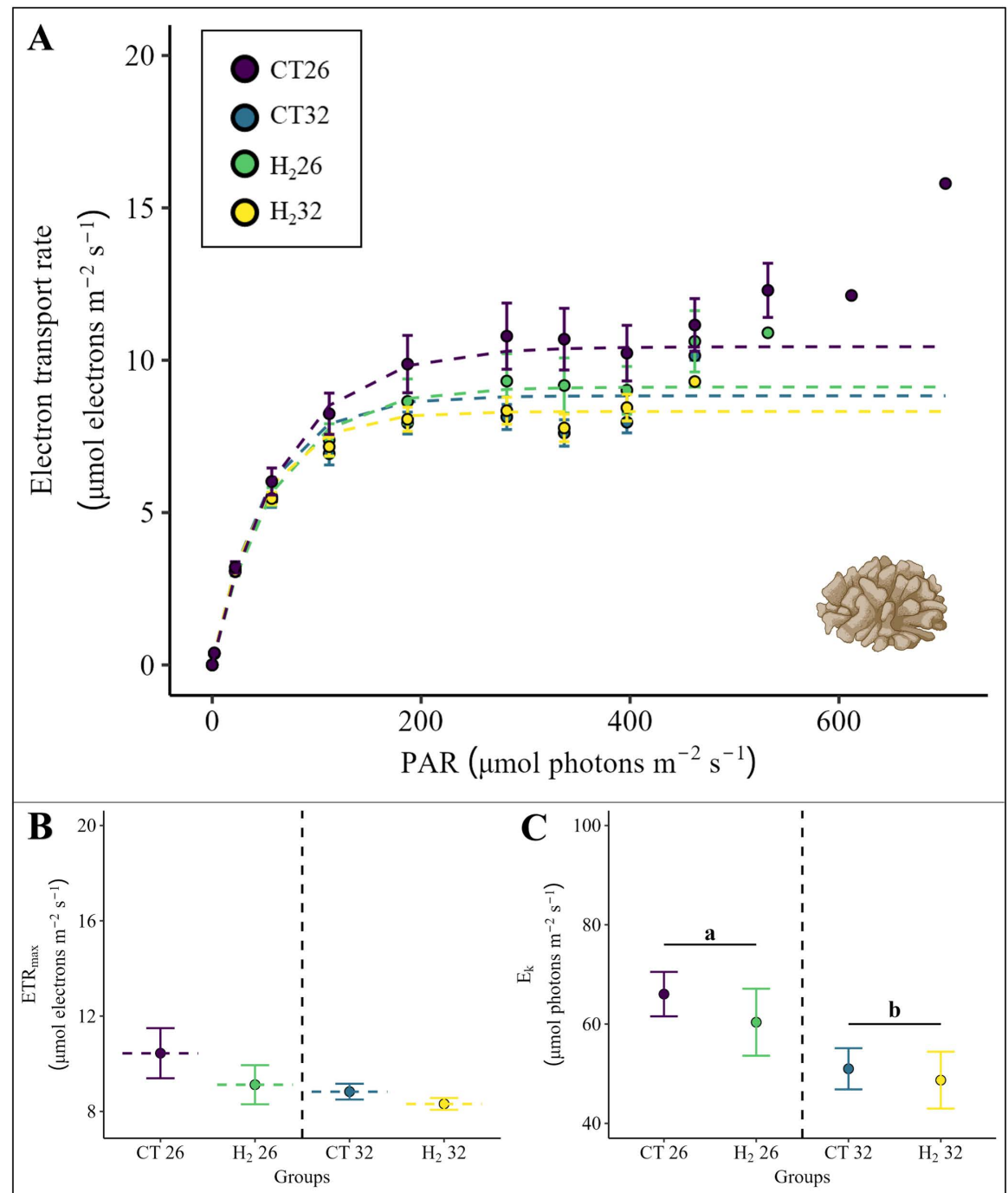
**Fig 4. (A) Rapid light curves, (B) maximum electron transport rates (ETR$_{max}$) and (C) minimum saturating irradiances (E$_k$) derived from the model fitted according to Platt et al. [42] for all four groups belonging to** *P. verrucosa*. The rapid light curves and the respective ETR$_{max}$ and E$_k$ values are calculated as the mean of six replicates per group (S1 File). The four groups are illustrated with different colors. Points indicate the mean value and error bars the respective standard error (SE). A significant temperature main effect according to the PERMANOVA with Monte-Carlo test (p < 0.05) is presented with letters and black lines grouping the temperature conditions. Exact p-values are presented in supplementary material (S1 File). Coral illustration was created with BioRender.com.

https://doi.org/10.1371/journal.pone.0308894.g004

## Symbiodiniaceae cell densities and chlorophyll concentrations

The Symbiodiniaceae cell density of *Acropora* sp. was significantly affected by temperature (Fig 5A, PERMANOVA, p = 0.047). Resembling the significant decline in photosynthetic efficiency, Symbiodiniaceae cell density of *Acropora* sp. decreased in both heat stress treatments (CT32 and $H_2$32) in comparison to the treatments at ambient temperature (CT26 and $H_2$26). However, chlorophyll a and c2 concentrations remained unaffected by temperature or treatment (Fig 5C and 5E).

While the Symbiodiniaceae cell density and chlorophyll a concentration of *P. verrucosa* was not significantly affected by temperature or treatment (Fig 5B and 5F), the areal chlorophyll $c_2$ concentration showed a significant effect of the hydrogen treatment (Fig 5D, PERMANOVA, p = 0.039). The addition of hydrogen ($H_2$26 and $H_2$32) resulted in a significant decrease of the areal chlorophyll $c_2$ concentration in comparison to both treatments without hydrogen addition (CT26 and CT32).

## Discussion

Coral reefs are currently experiencing the fourth global coral bleaching event [17,51], reaffirming the projections for an increase in both the scale and frequency of such events [10,15–17]. It is therefore crucial to deepen our understanding of the mechanisms driving coral bleaching [20] and to investigate new approaches to strengthen coral reefs, thereby potentially counteracting these events in the future [52,53]. In this context, molecular hydrogen might offer a promising approach since several studies have already demonstrated an extensive preventive and therapeutic effect of hydrogen in mammals including humans and rats [25–30]. Our study is the first to investigate the short-term effects of hydrogen on the ecophysiology of the coral holobiont under ambient temperatures and heat stress, providing insight into potential ecological implications.

### Molecular hydrogen can minimize negative effects of heat stress on the hard coral *Acropora* sp.

When under heat stress alone, *Acropora* sp. experienced a significant reduction in photosynthetic efficiency, $ETR_{max}$ and Symbiodiniaceae cell density alongside an increase in metabolic demand - indicative of a pronounced heat stress response [54,55]. However, simultaneous exposure to hydrogen and heat stress prevented the decline in the $ETR_{max}$ observed with heat stress alone in *Acropora* sp. As shown in previous studies, a decrease in $ETR_{max}$ can serve as an indicator of photosystem damage and a deteriorated health state of the Symbiodiniaceae cells [36,37,56]. This damage likely originates from the ROS/RNS accumulation under heat stress as proposed by the "Oxidative Theory" [20,23,24,57,58]. Our results therefore suggest that molecular hydrogen might have protected the coral holobiont from oxidative damage, thereby preventing a decrease in $ETR_{max}$. These findings align with the previously reported antioxidative capacity of molecular hydrogen [25–30]. In addition, molecular hydrogen may protect the photosynthetic apparatus indirectly by increasing antioxidant enzyme activity [59,60] and upregulating the heat shock response as observed in plants and rodents, respectively [33].

Consistent with our observations, a previous study in the Central Red Sea reported that *Acropora* sp. was more affected by simulated short-term heat stress than *P. verrucosa* [61]. This different response of *P. verrucosa* could indicate that the simulated heat stress was insufficient to induce negative effects within 48 h and suggests a higher temperature resistance in *P. verrucosa*, even though other studies have described *P. verrucosa* as more sensitive to temperature stress than *Acropora hemprichii* in the Red Sea [62]. The difference in the thermotolerance of the two investigated species may also be linked to the endosymbionts associated, as in
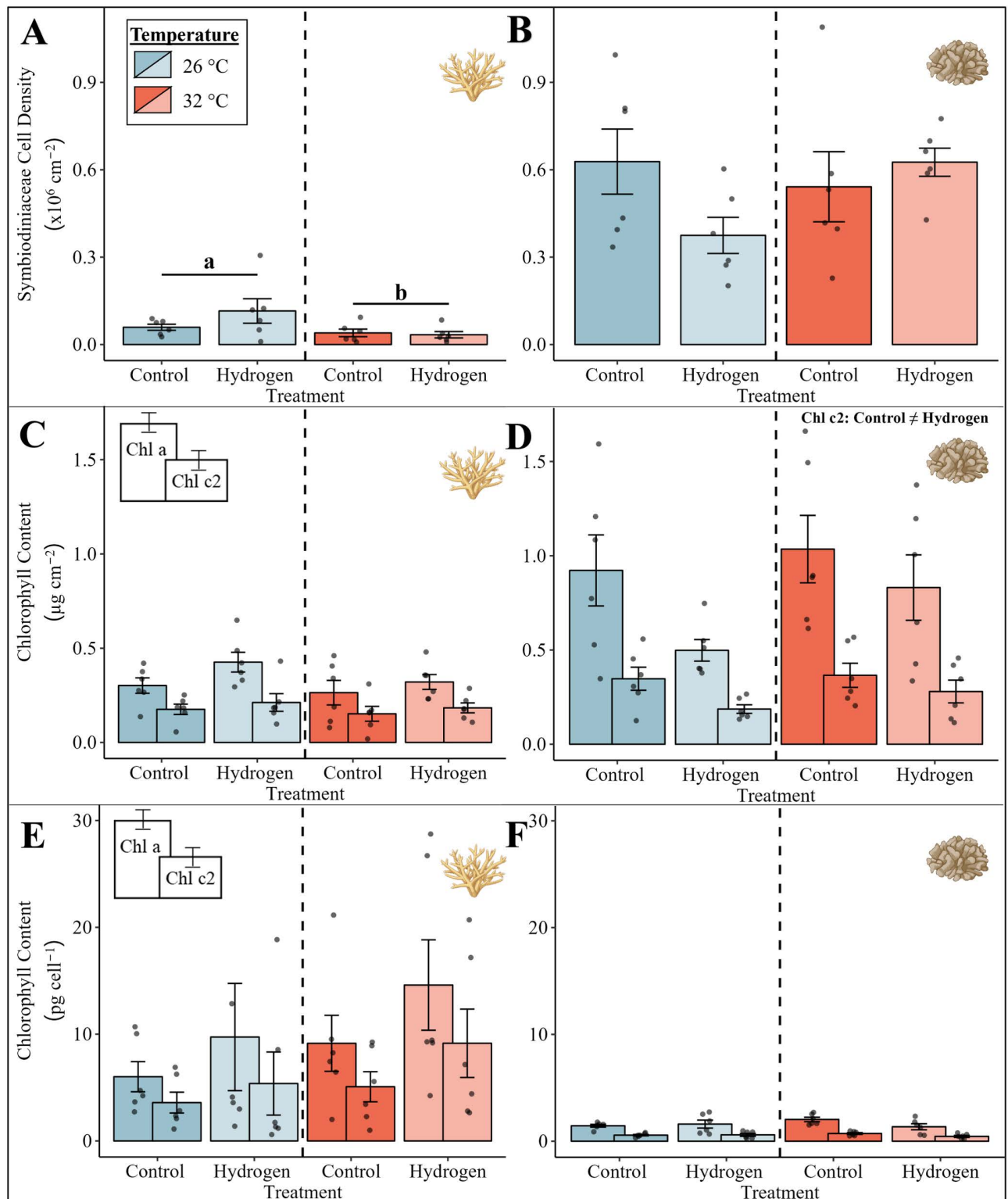
**Fig 5. Symbiodiniaceae cell density of (A)** *Acropora* **sp. and (B)** *P. verrucosa,* **areal chlorophyll content of (C)** *Acropora* **sp. and (D)** *P. verrucosa,* **and chlorophyll content per cell of (E)** *Acropora* **sp. and (F)** *P. verrucosa* **for the four groups.** Bars with error bars indicate the mean and the respective standard error (SE) of six replicates per group. For the chlorophyll content, chlorophyll a is presented on the left side of each bar with chlorophyll c2 at the right side. The color of the bars indicates the temperature condition (blue = 26 °C, red = 32 °C). A significant temperature main effect according to the PERMANOVA with Monte-Carlo test (p < 0.05) is presented with letters and black lines grouping the temperature conditions. A

significant treatment main effect according to the PERMANOVA with Monte-Carlo test (p < 0.05) is presented with the unequal sign in the top right corner. Exact p-values are presented in supplementary material (S1 File). Coral illustrations were created with BioRender.com.

https://doi.org/10.1371/journal.pone.0308894.g005

the Red Sea *Pocillopora* sp. is dominantly associated with *Symbiodinium* A1, while *Acropora* sp. mainly hosts *Symbiodinium* C41 [63].

## Molecular hydrogen negatively affects the photophysiology of *Acropora* sp. and *P. verrucosa* under ambient seawater temperatures

Contrary to our expectations, the addition of molecular hydrogen at ambient seawater temperatures resulted in a reversed effect in *Acropora* sp., significantly reducing the $ETR_{max}$ and $E_k$. Interestingly, hydrogen at ambient temperatures also led to a significant decrease of the respiration and photosynthesis rates as well as chlorophyll c2 concentrations in *P. verrucosa* together with the lowest Symbiodiniaceae cell densities and chlorophyll a concentrations, although these were not significant.

While supplementation with antioxidants can lead to detrimental effects - even resulting in mortality by potentially disrupting the balance of the antioxidative system [64,65] - hydrogen is generally regarded safe [29,66]. As molecular hydrogen selectively reduces the most harmful ROS and RNS, hydroxyl radicals and peroxynitrite, while not affecting other ROS and RNS that have a potential physiological role, hydrogen is considered as an ideal antioxidant [29].

We therefore propose a potential mechanism by which molecular hydrogen affects *Acropora* sp. and *P. verrucosa* under ambient seawater temperatures, presumably through the inhibition of nitrogen fixation in diazotrophs within the coral holobiont. Several *in vitro* studies have demonstrated that hydrogen competes with atmospheric nitrogen, thereby reducing the formation of bioavailable nitrogen, such as ammonium [67–70]. Under oligotrophic conditions, nitrogen fixation is critical for supplying bioavailable nitrogen [71,72] and therefore the inhibition could limit the overall nitrogen availability of the coral holobiont, particularly under ambient seawater temperatures, ultimately suppressing the photophysiology and growth of the coral holobiont [73–80]. Given the short generation time of Symbiodiniaceae, usually ranging from one to several days [81,82], a decreased growth rate may therefore explain an overall loss of Symbiodiniaceae cells in this short period. This may account for the lowest Symbiodiniaceae cell density and areal chlorophyll a concentration observed in *P. verrucosa* at ambient temperatures when exposed to molecular hydrogen, presumably associated with the significantly reduced photosynthesis rates and areal chlorophyll c2 concentrations. The variations between species might be correlated to differences in nitrogen fixation rates. Since nitrogen fixation rates were ~ 3-fold higher in *Acropora hemprichii* than in *P. verrucosa* [83], a partial inhibition of nitrogen fixation through the addition of hydrogen may have a greater impact on the already lower nitrogen fixation rates of *P. verrucosa*.

This theory is further supported by the temperature-dependent effects of hydrogen maintaining the photosynthesis and respiration rates of *P. verrucosa* under heat stress. At elevated temperatures, nitrogen fixation rates within the coral holobiont were shown to increase [84–86]. Consequently, the potentially reduced nitrogen fixation caused by molecular hydrogen [67–70] might help balance nitrogen availability, resulting in higher productivity compared to hydrogen addition at ambient temperatures. This scenario may even be beneficial under heat stress mitigating the risk of excessive endosymbiont proliferation [55] by maintaining a nitrogen-limited environment essential for the successful coral-algae symbiosis [19,22,86–88].

In contrast to this theory, Rädecker et al. [89] demonstrated that the ammonium produced by the increased nitrogen fixation rates under heat stress was not assimilated by the endosymbionts. Given these circumstances, the inhibitory effect of hydrogen may not support the endosymbionts under heat stress but potentially affect other microbial communities like nitrifiers and denitrifiers [22,90]. However, this theory remains speculative and future studies should address the effects of molecular hydrogen on nitrogen fixation and the bacterial community within the coral holobiont.
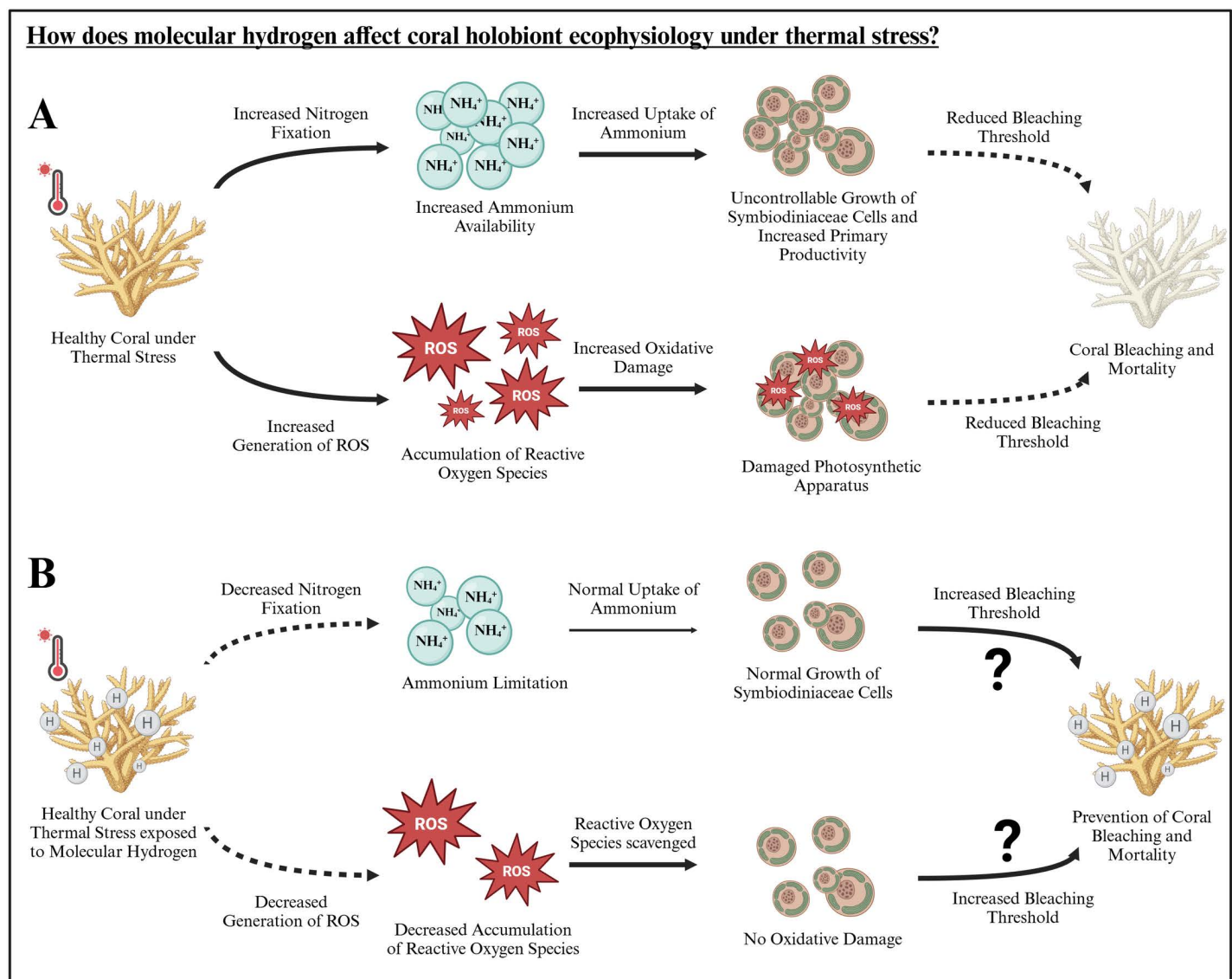


**Fig 6. Hypothesized effect of (A) heat stress and (B) heat stress in combination with molecular hydrogen on the coral holobiont ecophysiology.** First results indicate that hydrogen prevents oxidative damage of the photosystem of the Symbiodiniaceae cells. The potential mechanism of molecular hydrogen behind this effect is illustrated above with dotted lines indicating a decrease and bold lines indicating an increase in the respective process compared to each other. The question mark indicates a potential long-term effect which needs to be addressed in further studies (Illustration created with BioRender.com).

https://doi.org/10.1371/journal.pone.0308894.g006

## Ecological implications

Overall, our findings suggest that the effect of hydrogen addition on the coral holobiont is temperature-dependent. While hydrogen exposure had negatively affected the ecophysiology of *Acropora* sp. and *P. verrucosa* at ambient seawater temperatures, it showed a beneficial effect on the symbiont photophysiology of *Acropora* sp. under heat stress, indicating that molecular hydrogen is incorporated and potentially contributes to enhanced coral resilience under heat stress.

It is, however, important to acknowledge the study's limitations. The effects of molecular hydrogen were examined in only two hard coral species in the Central Red Sea and were limited to 48 h. Additionally, the experimental setup utilized a single tank for each treatment and species, designed specifically for treatment application rather than extended coral maintenance. While this design allowed precise and consistent environmental conditions and treatment addition, future long-term studies should aim to include an acclimatization phase and a greater number of tanks to mitigate potential tank effects over extended periods. Despite these limitations, our research offers initial evidence of the temperature-dependent effects of molecular hydrogen. Therefore, it can pave the way for future studies especially investigating following research questions: What specific mechanisms underlie molecular hydrogen's role in coral holobionts, particularly in relation to nitrogen fixation and oxidative damage (hypothesized mechanisms in Fig 6)? What are the long-term effects of molecular hydrogen on coral holobionts under both ambient and heat-stressed conditions?

If the hypothesized mechanisms of molecular hydrogen's effects on the coral holobiont are uncovered in future studies, it could offer invaluable insights into the mechanisms underlying coral bleaching potentially supporting the "Oxidative Theory" [23,24]. Further, this could lay the groundwork for the development of new tools in combat against coral bleaching, as ROS and RNS are not only involved in the cascades triggered by heat stress, but also by light stress, cold stress, high nitrate concentrations and bacterial infections [20]. However, careful consideration is needed regarding the safety and potential application of molecular hydrogen.

Given hydrogen's short retention time in water [91], the effects of molecular hydrogen on corals are presumably limited to the period immediately following administration preventing adverse effects at ambient seawater temperatures. Since hydrogen is a very small molecule rapidly diffusing across cell membranes [25], it is very likely that hydrogen will also affect other reef organisms. A recent study, for instance, demonstrated that hydrogen stimulates the growth of diverse marine bacteria [92]. Therefore, the effects of molecular hydrogen on the microbiome as well as other invertebrates and vertebrates, and the underlying mechanisms driving the enhanced thermal resistance, must be clarified prior to application.

With increasing interest in hydrogen as a potential emission-free and renewable energy carrier [26,93], extensive research has focused on developing simple methods for hydrogen production. Electrolysis devices converting distilled water or even seawater into molecular hydrogen are helping to make hydrogen widely available and affordable, thereby enhancing its potential in various applications [94,95]. Given the widespread abundance of hydrogen-producing bacteria [96] and their likely presence within the coral microbiome, identifying these bacteria could further reveal new beneficial microorganisms potentially supporting the development of effective probiotics [97–100].

To explore the full potential of molecular hydrogen, however, further research is essential. In particular, it is important to uncover the underlying temperature-dependent mechanisms, namely those associated with oxidative damage and nitrogen fixation, as well as establishing an optimal hydrogen concentration.

## Supporting information

**S1 File. Supplementary figures and statistical tables.**
(PDF)

**S1 Data. Supplementary data.**
(XLSX)

## Acknowledgments

## Author contributions

**Conceptualization:** Malte Ostendarp, Mareike de Breuyn, Yusuf C. El-Khaled, Raquel S. Peixoto, Christian Wild.

**Data curation:** Malte Ostendarp.

**Formal analysis:** Malte Ostendarp.

**Investigation:** Malte Ostendarp, Mareike de Breuyn.

**Methodology:** Malte Ostendarp, Mareike de Breuyn, Yusuf C. El-Khaled.

**Resources:** Yusuf C. El-Khaled, Neus Garcias-Bonet, Raquel S. Peixoto, Christian Wild.

**Software:** Malte Ostendarp.

**Supervision:** Yusuf C. El-Khaled, Raquel S. Peixoto, Christian Wild.

**Writing – original draft:** Malte Ostendarp.

**Writing – review & editing:** Malte Ostendarp, Mareike de Breuyn, Yusuf C. El-Khaled, Neus Garcias-Bonet, Susana Carvalho, Raquel S. Peixoto, Christian Wild.

## References

1. Brandl SJ, Rasher DB, Côté IM, Casey JM, Darling ES, Lefcheck JS, et al. Coral reef ecosystem functioning: eight core processes and the role of biodiversity. Frontiers in Ecol & Environ. 2019;17(8):445–54. https://doi.org/10.1002/fee.2088

2. Cinner J. Coral reef livelihoods. Current Opinion in Environmental Sustainability. 2014;7:65–71. https://doi.org/10.1016/j.cosust.2013.11.025

3. Bellwood DR, Hughes TP, Folke C, Nyström M. Confronting the coral reef crisis. Nature. 2004;429(6994):827–33. https://doi.org/10.1038/nature02691 PMID: 15215854

4. Wilkinson C. Status of coral reefs of the world: 2004. Townsville (Australia): Australian Institute of Marine Science (AIMS). 2004.

5. Roberts CM. Effects of Fishing on the Ecosystem Structure of Coral Reefs. Conserv Biol. 1995;9(5):988–95. https://doi.org/10.1046/j.1523-1739.1995.9051332.x-i1 PMID: 34261234

6. Dubinsky Z, Stambler N. Marine pollution and coral reefs. Global Change Biology. 1996;2(6):511–26. https://doi.org/10.1111/j.1365-2486.1996.tb00064.x

7. Hoegh-Guldberg O. Climate change, coral bleaching and the future of the world's coral reefs. Mar Freshwater Res. 1999. https://doi.org/10.1071/mf99078

8. Weil E, Smith G, Gil-Agudelo DL. Status and progress in coral reef disease research. Dis Aquat Organ. 2006;69(1):1–7. https://doi.org/10.3354/dao069001 PMID: 16703761

9. Pratchett M, Caballes C, Wilmes J, Matthews S, Mellin C, Sweatman H, et al. Thirty Years of Research on Crown-of-Thorns Starfish (1986–2016): Scientific Advances and Emerging Opportunities. Diversity. 2017;9(4):41. https://doi.org/10.3390/d9040041

10. Intergovernmental Panel on Climate Change (2022). Changing ocean, marine ecosystems, and dependent communities. The ocean and cryosphere in a changing climate: Special report of the intergovernmental panel on climate change. Cambridge University Press. 2022:447–588. https://doi.org/10.1017/9781009157964.007

11. Ripple WJ, Wolf C, Gregg JW, Rockström J, Newsome TM, Law BE, et al. The 2023 state of the climate report: Entering uncharted territory. BioScience. 2023;73(12):841–50. https://doi.org/10.1093/biosci/biad080

12. Li K, Zheng F, Cheng L, Zhang T, Zhu J. Record-breaking global temperature and crises with strong El Ni?o in 2023-2024. Innov Geo. 2023;1(2):100030. https://doi.org/10.59717/j.xinn-geo.2023.100030

13. Cheng L, Abraham J, Trenberth KE, Boyer T, Mann ME, Zhu J, et al. New Record Ocean Temperatures and Related Climate Indicators in 2023. Adv Atmos Sci. 2024;41(6):1068–82. https://doi.org/10.1007/s00376-024-3378-5

14. Li K, Zheng F, Zhu J, Zeng Q-C. El Niño and the AMO Sparked the Astonishingly Large Margin of Warming in the Global Mean Surface Temperature in 2023. Adv Atmos Sci. 2024;41(6):1017–22. https://doi.org/10.1007/s00376-023-3371-4

15. Emslie MJ, Logan M, Bray P, Ceccarelli DM, Cheal AJ, Hughes TP, et al. Increasing disturbance frequency undermines coral reef recovery. Ecological Monographs. 2024;94(3). https://doi.org/10.1002/ecm.1619

16. Mellin C, Brown S, Cantin N, Klein-Salas E, Mouillot D, Heron SF, et al. Cumulative risk of future bleaching for the world's coral reefs. Sci Adv. 2024;10(26):eadn9660. https://doi.org/10.1126/sciadv.adn9660 PMID: 38924396

17. National Oceanic and Atmospheric Administration. Daily global 5km satellite coral bleaching heat stress alert area. 2024 [cited 02 May 2024]. College Park, Maryland, USA: NOAA Coral Reef Watch. Available from: https://coralreefwatch.noaa.gov/product/5km/index_5km_baa-max-7d.php

18. Knowlton N, Corcoran E, Felis T, Ferse S, de Goeij J, Grottoli A, et al. Rebuilding Coral Reefs: A Decadal Grand Challenge. 2021. https://doi.org/10.53642/nrky9386

19. Wiedenmann J, D'Angelo C, Smith EG, Hunt AN, Legiret F-E, Postle AD, et al. Nutrient enrichment can increase the susceptibility of reef corals to bleaching. Nature Clim Change. 2012;3(2):160–4. https://doi.org/10.1038/nclimate1661

20. Helgoe J, Davy SK, Weis VM, Rodriguez-Lanetty M. Triggers, cascades, and endpoints: connecting the dots of coral bleaching mechanisms. Biol Rev Camb Philos Soc. 2024;99(3):715–52. https://doi.org/10.1111/brv.13042 PMID: 38217089

21. Dubinsky Z, Jokiel P. Ratio of energy and nutrient fluxes regulates symbiosis between zooxanthellae and corals. Pacific Science. 1994;48(3):313–24.

22. Rädecker N, Pogoreutz C, Voolstra CR, Wiedenmann J, Wild C. Nitrogen cycling in corals: the key to understanding holobiont functioning? Trends Microbiol. 2015;23(8):490–7. https://doi.org/10.1016/j.tim.2015.03.008 PMID: 25868684

23. Lesser MP, Stochaj WR, Tapley DW, Shick JM. Bleaching in coral reef anthozoans: effects of irradiance, ultraviolet radiation, and temperature on the activities of protective enzymes against active oxygen. Coral Reefs. 1990;8(4):225–32. https://doi.org/10.1007/bf00265015

24. Downs CA, Fauth JE, Halas JC, Dustan P, Bemiss J, Woodley CM. Oxidative stress and seasonal coral bleaching. Free Radic Biol Med. 2002;33(4):533–43. https://doi.org/10.1016/s0891-5849(02)00907-3 PMID: 12160935

25. Ohsawa I, Ishikawa M, Takahashi K, Watanabe M, Nishimaki K, Yamagata K, et al. Hydrogen acts as a therapeutic antioxidant by selectively reducing cytotoxic oxygen radicals. Nat Med. 2007;13(6):688–94. https://doi.org/10.1038/nm1577 PMID: 17486089

26. Huang C-S, Kawamura T, Toyoda Y, Nakao A. Recent advances in hydrogen research as a therapeutic medical gas. Free Radic Res. 2010;44(9):971–82. https://doi.org/10.3109/10715762.2010.500328 PMID: 20815764

27. Ito M, Ibi T, Sahashi K, Ichihara M, Ito M, Ohno K. Open-label trial and randomized, double-blind, placebo-controlled, crossover trial of hydrogen-enriched water for mitochondrial and inflammatory myopathies. Med Gas Res. 2011;1(1):24. https://doi.org/10.1186/2045-9912-1-24 PMID: 22146674

28. Ni X-X, Cai Z-Y, Fan D-F, Liu Y, Zhang R-J, Liu S-L, et al. Protective effect of hydrogen-rich saline on decompression sickness in rats. Aviat Space Environ Med. 2011;82(6):604–9. https://doi.org/10.3357/asem.2964.2011 PMID: 21702310

29. Ohta S. Molecular hydrogen as a preventive and therapeutic medical gas: initiation, development and potential of hydrogen medicine. Pharmacol Ther. 2014;144(1):1–11. https://doi.org/10.1016/j.pharmthera.2014.04.006 PMID: 24769081

30. Ishibashi T. Therapeutic Efficacy of Molecular Hydrogen: A New Mechanistic Insight. Curr Pharm Des. 2019;25(9):946–55. https://doi.org/10.2174/1381612825666190506123038 PMID: 31057105

31. Wu Q, Su N, Cai J, Shen Z, Cui J. Hydrogen-rich water enhances cadmium tolerance in Chinese cabbage by reducing cadmium uptake and increasing antioxidant capacities. J Plant Physiol. 2015;175:174–82. https://doi.org/10.1016/j.jplph.2014.09.017 PMID: 25543863

32. Jiang K, Kuang Y, Feng L, Liu Y, Wang S, Du H, et al. Molecular Hydrogen Maintains the Storage Quality of Chinese Chive through Improving Antioxidant Capacity. Plants (Basel). 2021;10(6):1095. https://doi.org/10.3390/plants10061095 PMID: 34072565

33. Nishiwaki H, Ito M, Negishi S, Sobue S, Ichihara M, Ohno K. Molecular hydrogen upregulates heat shock response and collagen biosynthesis, and downregulates cell cycles: meta-analyses of gene expression pro-files. Free Radic Res. 2018;52(4):434–45. https://doi.org/10.1080/10715762.2018.1439166 PMID: 29424253

34. Cziesielski MJ, Schmidt-Roach S, Aranda M. The past, present, and future of coral heat stress stud-ies. Ecol Evol. 2019;9(17):10055–66. https://doi.org/10.1002/ece3.5576 PMID: 31534713

35. Ralph PJ, Gademann R. Rapid light curves: A powerful tool to assess photosynthetic activity. Aquatic Botany. 2005;82(3):222–37. https://doi.org/10.1016/j.aquabot.2005.02.006

36. Bhagooli R, Hidaka M. Release of zooxanthellae with intact photosynthetic activity by the coral Galaxea fascicularis in response to high temperature stress. Marine Biology. 2004;145(2). https://doi.org/10.1007/s00227-004-1309-7

37. Bhagooli R, Hidaka M. Thermal inhibition and recovery of the maximum quantum yield of photosys-tem II and the maximum electron transport rate in zooxanthellae of a reef-building coral. Journal of the Japanese Coral Reef Society. 2006;8(1):1–11. https://doi.org/10.3755/jcrs.8.1

38. Lavy A, Eyal G, Neal B, Keren R, Loya Y, Ilan M. A quick, easy and non-intrusive method for under-water volume and surface area evaluation of benthic organisms by 3D computer modelling. Methods Ecol Evol. 2015;6(5):521–31. https://doi.org/10.1111/2041-210x.12331

39. Tilstra A, El-Khaled YC, Roth F, Rädecker N, Pogoreutz C, Voolstra CR, et al. Denitrification Aligns with N2 Fixation in Red Sea Corals. Sci Rep. 2019;9(1):19460. https://doi.org/10.1038/s41598-019-55408-z PMID: 31857601

40. Mezger SD, Klinke A, Tilstra A, El-Khaled YC, Thobor B, Wild C. The widely distributed soft coral Xenia umbellata exhibits high resistance against phosphate enrichment and temperature increase. Sci Rep. 2022;12(1):22135. https://doi.org/10.1038/s41598-022-26325-5 PMID: 36550166

41. Ralph PJ, Schreiber U, Gademann R, Kühl M, Larkum AWD. Coral photobiology studied with a new imaging pulse amplitude modulated fluorometer. Journal of Phycology. 2005;41(2):335–42. https://doi.org/10.1111/j.1529-8817.2005.04034.x

42. Platt T, Gallegos CL, Harrison WG. Photoinhibition of photosynthesis in natural assemblages of marine phytoplankton. J Mar Res. 1980; 38.

43. Silsbe GM, Malkin SY. Phytotools: Phytoplankton production tools. R package version 1.0. 2015.

44. R Development Core Team. R: A language and environment for statistical computing. (Vienna: R foundation for statistical computing). 2021.

45. Jeffrey SW, Humphrey GF. New spectrophotometric equations for determining chlorophylls a, b, c1 and c2 in higher plants, algae and natural phytoplankton. Biochemie und Physiologie der Pflanzen. 1975;167(2):191–4. https://doi.org/10.1016/s0015-3796(17)30778-3

46. Clarke KR, Gorley RN. PRIMER v6: Users manual/tutorial. 2006:1–192.

47. Anderson MJ. A new method for non-parametric multivariate analysis of variance. Austral Ecology. 2001;26(1):32–46. https://doi.org/10.1111/j.1442-9993.2001.01070.pp.x

48. Wickham H, Averick M, Bryan J, Chang W, McGowan L, François R, et al. Welcome to the Tidyverse. JOSS. 2019;4(43):1686. https://doi.org/10.21105/joss.01686

49. Kassambara A. *Ggpubr: 'Ggplot2' based publication ready plots. R package version 0.6.0.* 2023.

50. Kassambara A. *Rstatix: Pipe-friendly framework for basic statistical tests. R package version 0.7.2.* 2023.

51. Reimer JD, Peixoto RS, Davies SW, Traylor-Knowles N, Short ML, Cabral-Tena RA, et al. The Fourth Global Coral Bleaching Event: Where do we go from here? Coral Reefs. 2024;43(4):1121–5. https://doi.org/10.1007/s00338-024-02504-w

52. Kleypas J, Allemand D, Anthony K, Baker AC, Beck MW, Hale LZ, et al. Designing a blueprint for coral reef survival. Biological Conservation. 2021;257:109107. https://doi.org/10.1016/j.biocon.2021.109107

53. Voolstra CR, Suggett DJ, Peixoto RS, Parkinson JE, Quigley KM, Silveira CB, et al. Extending the natural adaptive capacity of coral holobionts. Nat Rev Earth Environ. 2021;2(11):747–62. https://doi.org/10.1038/s43017-021-00214-3

54. Figueroa FL, Bonomi-Barufi J, Celis-Plá PSM, Nitschke U, Arenas F, Connan S, et al. Short-term effects of increased CO2, nitrate and temperature on photosynthetic activity in Ulva rigida (Chlorophyta) estimated by different pulse amplitude modulated fluorometers and oxygen evolution. J Exp Bot. 2021;72(2):491–509. https://doi.org/10.1093/jxb/eraa473 PMID: 33064811

55. Rädecker N, Pogoreutz C, Gegner HM, Cárdenas A, Roth F, Bougoure J, et al. Heat stress destabilizes symbiotic nutrient cycling in corals. Proc Natl Acad Sci U S A. 2021;118(5):e2022653118. https://doi.org/10.1073/pnas.2022653118 PMID: 33500354

56. Ferrier-Pagès C, Rottier C, Beraud E, Levy O. Experimental assessment of the feeding effort of three scleractinian coral species during a thermal stress: Effect on the rates of photosynthesis. Journal of Experimental Marine Biology and Ecology. 2010;390(2):118–24. https://doi.org/10.1016/j.jembe.2010.05.007

57. Brown BE. Coral bleaching: causes and consequences. Coral Reefs. 1997;16(0):S129–38. https://doi.org/10.1007/s003380050249

58. Higuchi T, Fujimura H, Hitomi Y, Arakaki T, Oomori T, Suzuki Y. Photochemical formation of hydroxyl radicals in tissue extracts of the coral Galaxea fascicularis. Photochem Photobiol. 2010;86(6):1421–6. https://doi.org/10.1111/j.1751-1097.2010.00802.x PMID: 21155074

59. Jin Q, Zhu K, Cui W, Xie Y, Han B, Shen W. Hydrogen gas acts as a novel bioactive molecule in enhancing plant tolerance to paraquat-induced oxidative stress via the modulation of heme oxygenase-1 signalling system. Plant Cell Environ. 2013;36(5):956–69. https://doi.org/10.1111/pce.12029 PMID: 23094798

60. Zhang X, Zhao X, Wang Z, Shen W, Xu X. Protective effects of hydrogen-rich water on the photosynthetic apparatus of maize seedlings (Zea mays L.) as a result of an increase in antioxidant enzyme activities under high light stress. Plant Growth Regul. 2015;77(1):43–56. https://doi.org/10.1007/s10725-015-0033-2

61. de Breuyn M, Ostendarp M, El-Khaled YC, Garcias-Bonet N, Carvalho S, Wild C, et al. Probiotics prevent mortality of thermal-sensitive corals exposed to short-term heat stress. ISME Commun. 2025. *Accepted*.

62. Evensen NR, Voolstra CR, Fine M, Perna G, Buitrago-López C, Cárdenas A, et al. Empirically derived thermal thresholds of four coral species along the Red Sea using a portable and standardized experimental approach. Coral Reefs. 2022;41(2):239–52. https://doi.org/10.1007/s00338-022-02233-y

63. Ziegler M, Arif C, Burt JA, Dobretsov S, Roder C, LaJeunesse TC, et al. Biogeography and molecular diversity of coral symbionts in the genus Symbiodinium around the Arabian Peninsula. J Biogeogr. 2017;44(3):674–86. https://doi.org/10.1111/jbi.12913 PMID: 28286360

64. Villanueva C, Kross RD. Antioxidant-induced stress. Int J Mol Sci. 2012;13(2):2091–109. https://doi.org/10.3390/ijms13022091 PMID: 22408440

65. Dungan AM, Maire J, Perez-Gonzalez A, Blackall LL, van Oppen MJH. Lack of evidence for the oxidative stress theory of bleaching in the sea anemone, Exaiptasia diaphana, under elevated temperature. Coral Reefs. 2022;41(4):1161–72. https://doi.org/10.1007/s00338-022-02251-w

66. Johnsen HM, Hiorth M, Klaveness J. Molecular Hydrogen Therapy-A Review on Clinical Studies and Outcomes. Molecules. 2023;28(23):7785. https://doi.org/10.3390/molecules28237785 PMID: 38067515

67. Wilson PW, Umbreit WW. Mechanism of symbiotic nitrogen fixation. Archiv Mikrobiol. 1937;8(1–4):440–57. https://doi.org/10.1007/bf00407213

68. Hwang JC, Chen CH, Burris RH. Inhibition of nitrogenase-catalyzed reductions. Biochim Biophys Acta. 1973;292(1):256–70. https://doi.org/10.1016/0005-2728(73)90270-3 PMID: 4705133

69. Burgess BK, Wherland S, Newton WE, Stiefel EI. Nitrogenase reactivity: insight into the nitrogen-fixing process through hydrogen-inhibition and HD-forming reactions. Biochemistry. 1981;20(18):5140–6. https://doi.org/10.1021/bi00521a007 PMID: 6945872

70. Guth JH, Burris RH. Inhibition of nitrogenase-catalyzed NH3 formation by H2. Biochemistry. 1983;22(22):5111–22. https://doi.org/10.1021/bi00291a010 PMID: 6360203

71. Cardini U, Bednarz VN, Naumann MS, van Hoytema N, Rix L, Foster RA, et al. Functional significance of dinitrogen fixation in sustaining coral productivity under oligotrophic conditions. Proc Biol Sci. 2015;282(1818):20152257. https://doi.org/10.1098/rspb.2015.2257 PMID: 26511052

72. Lesser MP, Morrow KM, Pankey MS. N2 fixation, and the relative contribution of fixed N, in corals from Curaçao and Hawaii. Coral Reefs. 2019;38(6):1145–58. https://doi.org/10.1007/s00338-019-01863-z

73. Howarth RW. Nutrient limitation of net primary production in marine ecosystems. Annu Rev Ecol Syst. 1988;19(1):89–110. https://doi.org/10.1146/annurev.es.19.110188.000513

74. Williams S, Carpenter R. Nitrogen-limited primary productivity of coral reef algal turfs: potential contribution of ammonium excreted by Diadema antillarum. Mar Ecol Prog Ser. 1988;47:145–52. https://doi.org/10.3354/meps047145

75. Hatcher BG. Coral reef primary productivity. A hierarchy of pattern and process. Trends Ecol Evol. 1990;5(5):149–55. https://doi.org/10.1016/0169-5347(90)90221-X PMID: 21232343

76. Falkowski PG, Dubinsky Z, Muscatine L, McCloskey L. Population Control in Symbiotic Corals. BioScience. 1993;43(9):606–11. https://doi.org/10.2307/1312147

77. Ferrier-Pagès C, Gattuso J-P, Dallot S, Jaubert J. Effect of nutrient enrichment on growth and photosynthesis of the zooxanthellate coral Stylophora pistillata. Coral Reefs. 2000;19(2):103–13. https://doi.org/10.1007/s003380000078

78. Krueger T, Horwitz N, Bodin J, Giovani M-E, Escrig S, Fine M, et al. Intracellular competition for nitrogen controls dinoflagellate population density in corals. Proc Biol Sci. 2020;287(1922):20200049. https://doi.org/10.1098/rspb.2020.0049 PMID: 32126963

79. Roberty S, Béraud E, Grover R, Ferrier-Pagès C. Coral Productivity Is Co-Limited by Bicarbonate and Ammonium Availability. Microorganisms. 2020;8(5):640. https://doi.org/10.3390/microorganisms8050640 PMID: 32354088

80. Zhou Z, Zhang K, Wang L, Su Y, Wang J, Song T, et al. Nitrogen availability improves the physiological resilience of coral endosymbiont Cladocopium goreaui to high temperature. J Phycol. 2021;57(4):1187–98. https://doi.org/10.1111/jpy.13156 PMID: 33650119

81. Sammarco PW, Strychar KB. Effects of Climate Change/Global Warming on Coral Reefs: Adaptation/Exaptation in Corals, Evolution in Zooxanthellae, and Biogeographic Shifts. Environmental Bioindicators. 2009;4(1):9–45. https://doi.org/10.1080/15555270902905377

82. Chakravarti LJ, van Oppen MJH. Experimental Evolution in Coral Photosymbionts as a Tool to Increase Thermal Tolerance. Front Mar Sci. 2018;5. https://doi.org/10.3389/fmars.2018.00227

83. El-Khaled YC, Roth F, Rädecker N, Tilstra A, Karcher DB, Kürten B, et al. Nitrogen fixation and denitrification activity differ between coral- and algae-dominated Red Sea reefs. Sci Rep. 2021;11(1):11820. https://doi.org/10.1038/s41598-021-90204-8 PMID: 34083565

84. Cardini U, Bednarz VN, Foster RA, Wild C. Benthic N2 fixation in coral reefs and the potential effects of human-induced environmental change. Ecol Evol. 2014;4(9):1706–27. https://doi.org/10.1002/ece3.1050 PMID: 24967086

85. Santos HF, Carmo FL, Duarte G, Dini-Andreote F, Castro CB, Rosado AS, et al. Climate change affects key nitrogen-fixing bacterial populations on coral reefs. ISME J. 2014;8(11):2272–9. https://doi.org/10.1038/ismej.2014.70 PMID: 24830827

86. Cardini U, van Hoytema N, Bednarz VN, Rix L, Foster RA, Al-Rshaidat MMD, et al. Microbial dinitrogen fixation in coral holobionts exposed to thermal stress and bleaching. Environ Microbiol. 2016;18(8):2620–33. https://doi.org/10.1111/1462-2920.13385 PMID: 27234003

87. Pogoreutz C, Rädecker N, Cárdenas A, Gärdes A, Voolstra CR, Wild C. Sugar enrichment provides evidence for a role of nitrogen fixation in coral bleaching. Glob Chang Biol. 2017;23(9):3838–48. https://doi.org/10.1111/gcb.13695 PMID: 28429531

88. Thobor B, Tilstra A, Bourne DG, Springer K, Mezger SD, Struck U, et al. The pulsating soft coral Xenia umbellata shows high resistance to warming when nitrate concentrations are low. Sci Rep. 2022;12(1):16788. https://doi.org/10.1038/s41598-022-21110-w PMID: 36202937

89. Rädecker N, Pogoreutz C, Gegner HM, Cárdenas A, Perna G, Geißler L, et al. Heat stress reduces the contribution of diazotrophs to coral holobiont nitrogen cycling. ISME J. 2022;16(4):1110–8. https://doi.org/10.1038/s41396-021-01158-8 PMID: 34857934

90. El-Khaled YC, Nafeh R, Roth F, Rädecker N, Karcher DB, Jones BH, et al. High plasticity of nitrogen fixation and denitrification of common coral reef substrates in response to nitrate availability. Mar Pollut Bull. 2021;168:112430. https://doi.org/10.1016/j.marpolbul.2021.112430 PMID: 34000709

91. Zhao G, Cheng P, Zhang T, Abdalmegeed D, Xu S, Shen W. Hydrogen-rich water prepared by ammonia borane can enhance rapeseed (Brassica napus L.) seedlings tolerance against salinity, drought or cadmium. Ecotoxicol Environ Saf. 2021;224:112640. https://doi.org/10.1016/j.ecoenv.2021.112640 PMID: 34392154

92. Lappan R, Shelley G, Islam ZF, Leung PM, Lockwood S, Nauer PA, et al. Molecular hydrogen in seawater supports growth of diverse marine bacteria. Nat Microbiol. 2023;8(4):581–95. https://doi.org/10.1038/s41564-023-01322-0 PMID: 36747116

93. Najjar YSH. Hydrogen safety: The road toward green technology. International Journal of Hydrogen Energy. 2013;38(25):10716–28. https://doi.org/10.1016/j.ijhydene.2013.05.126

94. Mohammed-Ibrahim J, Moussab H. Recent advances on hydrogen production through seawater electrolysis. Materials Science for Energy Technologies. 2020;3:780–807. https://doi.org/10.1016/j.mset.2020.09.005

95. Saeedi Zadegan M, Zamani Pedram M, Sohani A, Hoseinzadeh S. A super-efficient method for hydrogen production from seawater. International Journal of Hydrogen Energy. 2022;47(62):26135–55. https://doi.org/10.1016/j.ijhydene.2022.04.122

96. Hallenbeck PC, Liu Y. Recent advances in hydrogen production by photosynthetic bacteria. International Journal of Hydrogen Energy. 2016;41(7):4446–54. https://doi.org/10.1016/j.ijhydene.2015.11.090

97. Rosado PM, Leite DCA, Duarte GAS, Chaloub RM, Jospin G, Nunes da Rocha U, et al. Marine probiotics: increasing coral resistance to bleaching through microbiome manipulation. ISME J. 2019;13(4):921–36. https://doi.org/10.1038/s41396-018-0323-6 PMID: 30518818

98. van Oppen MJH, Blackall LL. Coral microbiome dynamics, functions and design in a changing world. Nat Rev Microbiol. 2019;17(9):557–67. https://doi.org/10.1038/s41579-019-0223-4 PMID: 31263246

99. Peixoto RS, Sweet M, Villela HDM, Cardoso P, Thomas T, Voolstra CR, et al. Coral Probiotics: Premise, Promise, Prospects. Annu Rev Anim Biosci. 2021;9:265–88. https://doi.org/10.1146/annurev-animal-090120-115444 PMID: 33321044

100. Delgadillo-Ordoñez N, Garcias-Bonet N, Raimundo I, García FC, Villela H, Osman EO, et al. Probiotics reshape the coral microbiome in situ without detectable off-target effects in the surrounding environment. Commun Biol. 2024;7(1):434. https://doi.org/10.1038/s42003-024-06135-3 PMID: 38594357